DYNAMIC RESPONSE OF AN ELASTIC ICE SHEET TO THE EXCITATION OF ITS BOUNDARY EDGE

J. Kajaste-Rudnitski

Rakenteiden Mekaniikka Vol. 21
No 4 1989, s. 25...60

Abstract

In the process of ice-structure interaction, elastic waves propagate outward from the contact points into the depth of a moving infinite ice sheet carrying with them a certain amount of energy. Althouhg the equations of motion do not contain dissipative terms, the damping effect occurs due to the border geometry. If not taken into account, this geometrical damping can cause substantial errors in the load evaluation.

To demonstrate a phenomenon, the method of potentials is used to solve a dynamic problem of the elastic half-plane subjected to the arbitrary force acting on its boundary edge.

This research was carried out as part of a joint project in cooperation with the Norwegian Geotechnical Institute, Oslo, Norway.

1 Introduction

As a result of extensive research in the area of Arctic offsore technolgy, a number of ice-structure interaction models were introduced. Due to different points of view on the same problem, these models are divided into two main groups according to the following concepts: the negative damping and self excitation (Määttänen, 1988) for one and characteristic failure frequency (Sodhi, 1988) for another. Although both concepts are based on the field measurements and laboratory tests data, there exist certain contradictions between them and each claims to be the right one.

As an attempt to reconcile these two concepts, a new analytical model for ice induced vibrations of slender structures has recently been

developed (Kärnä & Turunen, 1989). Its specific features are a highly non-linear-one-dirction spring between ice and structure and a geometrical damping of the ice sheet due to energy dissipation with outgoing elastic shock waves.

A dynamic behaviour of the ice sheet considered as a half plane is studied, below.

2 Displacement potentials

A displacement vector field $u(u_1,u_2,u_3)$ may be expressed in terms of one scalar function Φ and a vector field $\psi(\psi_1,\psi_2,\psi_3)$ which are called a scalar and a vector potential respectively.

$$u_i = \Phi_{,i} + e_{ijk}\psi_{k,j} \tag{1}$$

The expression (1) makes a divergence $\psi_{i,j}$ arbitrary, and it is further assumed to be zero.

Putting (1) into Navier equation of motion

$$\rho \frac{\partial^2}{\partial t^2} u_i = Gu_{i,jj} + (\lambda + G)u_{j,ji} \tag{2}$$

one will have

$$\rho \frac{\partial^2}{\partial t^2} \Phi_{,i} + \rho e_{ijk} \frac{\partial^2}{\partial t^2} \psi_{k,j} = (\lambda + G) \frac{\partial}{\partial x_i} \Delta\Phi + G \frac{\partial}{\partial x_i} \Delta\Phi + Ge_{ijk} \frac{\partial}{\partial x_j} \Delta\psi \tag{3}$$

where Δ is a Laplacian and λ and G are Lamé constants. The density ρ is a constant.

If the functions Φ and ψ_i are solutions of the wave equations

$$\Delta\Phi = \frac{1}{C_L^2}\frac{\partial^2}{\partial t^2}\Phi \quad \text{and} \quad \Delta\psi_k = \frac{1}{C_T^2}\frac{\partial^2}{\partial t^2}\psi_k \tag{4}$$

the equation (3) will be satisfied. Constants C_L and C_T are velocities of the dilatational and distortional waves respectively.

$$C_L = \sqrt{\frac{\lambda + 2G}{\rho}} \quad \text{and} \quad C_T = \sqrt{\frac{G}{\rho}} \tag{5}$$

3 Impulse function for a half-plane

Consider an elastic half-plane in a coordinate system z - x with an unit impulse force applied to the origin at the time moment t = 0.

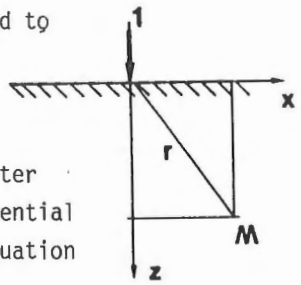

It is assumed that there are no out-of-plane rotations and, that the plane remains plane after deformation. It means that only one vector potential is required. In an actual coordinate system equation (1) can be rewritten

$$u = \frac{\partial\Phi}{\partial x} - \frac{\partial\psi}{\partial z} \quad ; \quad w = \frac{\partial\Phi}{\partial z} + \frac{\partial\psi}{\partial x} \tag{6}$$

and the wave equations (4) look as follows:

$$\left(\frac{\partial^2}{\partial x^2} + \frac{\partial^2}{\partial z^2}\right)\Phi = \frac{1}{C_L^2}\frac{\partial^2}{\partial t^2}\Phi$$

$$\left(\frac{\partial^2}{\partial x^2} + \frac{\partial^2}{\partial z^2}\right)\psi = \frac{1}{C_T^2}\frac{\partial^2}{\partial t^2}\psi \qquad (7)$$

For a plane stress state the Hook law and a strain tensor are

$$\sigma_{ij} = \frac{\lambda(1 - 2\mu)}{1 - \mu} e_{kk}\delta_{ij} + 2Ge_{ij}$$

$$e_{ij} = \frac{1}{2}(u_{i,j} + u_{j,i}) \qquad (8)$$

with μ as a Poisson ratio and a factor $\frac{(1 - 2\mu)}{1 - \mu}$ as a consequence of $\sigma_{yy} = 0$.

Having in mind relations (6) the stress components can be derived from (8) in the actual coordinate system

$$\sigma_{zz} = \frac{\lambda(1 - 2\mu)}{1 - \mu}\Delta\Phi + 2G\left(\frac{\partial^2}{\partial z^2}\Phi + \frac{\partial^2}{\partial x \partial z}\psi\right)$$

$$\sigma_{xx} = \frac{\lambda(1 - 2\mu)}{1 - \mu}\Delta\Phi + 2G\left(\frac{\partial^2}{\partial x^2}\Phi - \frac{\partial^2}{\partial z \partial x}\psi\right) \qquad (9)$$

$$\sigma_{xz} = G\left(2\frac{\partial^2}{\partial x \partial z}\Phi + \frac{\partial^2}{\partial x^2}\psi - \frac{\partial^2}{\partial z^2}\psi\right)$$

The boundary edge is free of stresses all the time except at the point (0,0) where at t = 0 unit impulse is applied.

$$\sigma_{zx} = 0 \quad ; \quad \sigma_{zz}\Big|_{z=0} = -\delta(x,t) \tag{10}$$

Here $\delta(x,t)$ is a two dimensional Dirac delta-function such that

$$\int_{-\infty}^{\infty}\int \delta(x,t)\, dxdt = 1 \tag{11}$$

It is equivalent to the concentrated load of unit magnitude applied to the point (0,0) at $t = 0$ and vanishes for all $t > 0$. Without changing the meaning of (11) $\delta(x,t)$ can be presented as a product of two one-dimensional delta functions $\delta(x,t) = \delta(x)\,\delta(t)$. Further on, the solution of the equation (7) with boundary conditions (10) is sought following the Cagniard method (Fung, 1965). First the equations (7) are transformed by Laplace transformation with respect to time.

$$\Delta\bar{\Phi} = \frac{s^2}{C_L^2}\bar{\Phi} \quad \text{and} \quad \Delta\bar{\psi} = \frac{s^2}{C_T^2}\bar{\psi} \tag{12}$$

The same is done with the boundary conditions (10)

$$\begin{aligned} &2\frac{\partial^2}{\partial x \partial z}\bar{\Phi} + \frac{\partial^2}{\partial x^2}\bar{\psi} - \frac{\partial^2}{\partial z^2}\bar{\psi} = 0 \\ &\lambda\frac{(1-2\mu)}{1-\mu}\Delta\bar{\Phi} + 2G\left(\frac{\partial^2}{\partial z^2}\bar{\Phi} + \frac{\partial^2}{\partial x \partial z}\bar{\psi}\right) = -\delta(x) \end{aligned} \tag{13}$$

Note that the Laplace transform of $\delta(t)$ is a unity and $\bar{\Phi}$ and $\bar{\psi}$ are transforms of Φ and ψ respectively.

It is easily verified by substitution that the following functions are solutions of (12)

$$\bar{\Phi} = \exp(iksx - sz\sqrt{k^2 + v_1^2})$$

$$\bar{\psi} = \exp(iksx - sz\sqrt{k^2 + v_2^2}) \tag{14}$$

providing that $v_1 = 1/C_L$ and $v_2 = 1/C_T$. Here $i = \sqrt{-1}$ and k is a real variable.

The general solution of (12) can be written in the form of curvilinear integrals

$$\bar{\Phi} = \int_\Gamma P_1(k) \exp[-s\,(z\sqrt{v_1^2 + k^2} - ikx)]dk$$

$$\bar{\psi} = \int_\Gamma P_2(k) \exp[-s\,(z\sqrt{v_2^2 + k^2} - ikx)]dk \tag{15}$$

with an integration path Γ along the positive direction of a real k-axis. Two arbitrary functions $P_1(k)$ and $P_2(k)$ will be chosen in a way to satisfy the boundary conditions (13). To ensure the convergence of (15) when $z \to \infty$ the real parts of square roots should be positive.

After substituting (15) into (13) two equations emerge

$$\int_\Gamma [-2ik\sqrt{v_1^2 + k^2}\, P_1(k) - (2k^2 + v_2^2)P_2(k)]s^2 \exp(iksx)dk = 0 \tag{16}$$

$$\int_\Gamma [(2k^2 + \frac{1 - 2\mu}{(1 - \mu)^2} v_2^2)\, P_1(k) - 2ik\sqrt{v_2^2 + k^2}\, P_2(k)]$$

$$Gs^2 \exp(iksx)dk = -\delta(x) \tag{17}$$

Equation (16) will be satisfied if $P_1(k) = (2k^2 + v_2^2)R(k)$ and $P_2(k) = -2ik\sqrt{v_1^2 + k^2}\, R(k)$. A new unknown function R(k) can be found from (17).

$$\int_{\Gamma}[(2k^2 + \frac{1-2\mu}{(1-\mu)^2} v_2^2)(2k^2 + v_2^2) - 4k^2\sqrt{(k^2+v_1^2)(k^2+v_2^2)}] \cdot R(k)dk = -\delta(x) \tag{18}$$

Dirac delta-function in (18) should be presented in a form of Fourier integral. To do so consider the delta-function as a limit of a square-wave

$$\lim_{\epsilon\to 0} \frac{1}{\epsilon}[U(x+\frac{\epsilon}{2}) - U(x-\frac{\epsilon}{2})] \tag{19}$$

where U(x) is a unit step-function which itself can be regarded as a limit of $\exp(-\beta x)\,U(x)$ when $\beta \to 0$.

$$\delta(x) = \lim_{\substack{\epsilon\to 0\\ \beta\to 0}} \frac{1}{2\pi\epsilon} \int_{-\infty}^{\infty} e^{ikx}\,dk \int_{-\infty}^{\infty}[e^{-\beta(\zeta+\frac{\epsilon}{2})} - e^{-\beta(\zeta-\frac{\epsilon}{2})}]\,e^{-ik\zeta}\,d\zeta$$

$$= \lim_{\substack{\epsilon\to 0\\ \beta\to 0}} \frac{1}{2\pi\epsilon} \int_{-\infty}^{\infty} e^{ikx}\,[\int_{-\frac{\epsilon}{2}}^{\infty} e^{-\beta(\zeta+\frac{\epsilon}{2})}\,e^{-ik\zeta}\,d\zeta - \int_{\frac{\epsilon}{2}}^{\infty} e^{-\beta(\zeta-\frac{\epsilon}{2})}\,e^{-ik\zeta}\,d\zeta]dk$$

$$= \lim_{\substack{\epsilon\to 0\\ \beta\to 0}} \frac{1}{2\pi} \int_{-\infty}^{\infty} e^{ikx} \frac{i}{\frac{\epsilon\beta}{2} + \frac{i\epsilon k}{2}} \sin\frac{\epsilon k}{2}\,dk = \frac{1}{2\pi}\int_{-\infty}^{\infty} e^{ikx}\,dk$$

Parameter s can be easily incorporated into this integral so that

$$\delta(x) = \frac{s}{2\pi}\int_{\Gamma} e^{iksx}\,dk \tag{20}$$

Now to satisfy (18) an unknown function R(k) must be as follows

$$R(k) = -\frac{s}{2\pi Gs}\,\frac{1}{(2k^2 + \alpha v_2^2)(2k^2 + v_2^2) - 4k^2\sqrt{(k^2 + v_1^2)(k^2 + v_2^2)}}.$$

with $\alpha = \dfrac{1 - 2\mu}{(1 - \mu)^2}$

Finally the transforms of potential functions (15) take a form

$$\begin{aligned}\bar{\Phi} &= -\frac{1}{2\pi Gs}\int_\Gamma \frac{2k^2 + v_2^2}{\Delta(k)}\exp\left[-s(\sqrt{v_1^2 + k^2}\cdot z - ikx)\right]dk \\ \bar{\psi} &= \frac{1}{2\pi Gs}\int_\Gamma \frac{2ik\sqrt{v_1^2 + k^2}}{\Delta(k)}\exp\left[-s(\sqrt{v_2^2 + k^2}\cdot z - ikx)\right]dk\end{aligned} \tag{21}$$

and transforms of displacement functions are

$$\begin{aligned}\bar{u} &= \frac{i}{2\pi G}\left[-\int_\Gamma \frac{k(2k^2 + v_2^2)}{\Delta(k)}e^{\zeta}\,dk + \int_\Gamma \frac{2k\sqrt{v_1^2 + k^2}\sqrt{v_2^2 + k^2}}{\Delta(k)}e^{\eta}\,dk\right] \\ \bar{w} &= \frac{1}{2\pi G}\left[\int_\Gamma \frac{(2k^2 + v_2^2)\sqrt{v_1^2 + k^2}}{\Delta(k)}e^{\zeta}\,dk - \int_\Gamma \frac{2k^2\sqrt{v_1^2 + k^2}}{\Delta(k)}e^{\eta}\,dk\right]\end{aligned} \tag{22}$$

where $\Delta(k) = (2k^2 + \alpha v_2^2)(2k^2 + v_2^2) - 4k^2\sqrt{(k^2 + v_1^2)(k^2 + v_2^2)}$

$$\begin{aligned}\zeta &= -s\sqrt{v_1^2 + k^2}\cdot z + iskx = -s(\sqrt{v_1^2 + k^2}\cdot z - ikx) \\ \eta &= -s\sqrt{v_2^2 + k^2}\cdot z + iskz = -s(\sqrt{v_2^2 + k^2}\cdot z - ikx)\end{aligned} \tag{22*}$$

Now consider the variable k as a complex one. The integrals in (22) are now on the whole k-plane with the path of integration along the real axis. Introducing a formal substitution

$$\sqrt{k^2 + v_1^2} \cdot z - ikx = t \qquad (23)$$

and deforming the path of integration Γ into another path Γ_1 so that the integration on t-plane will be along a positive real axis from 0 to ∞ the integrals in (22) will take a form of direct Laplace transformation

$$\int_0^\infty F(x,z,t)\, e^{-st}\, dt \qquad (24)$$

and F(x,z,t) is recognized as an original function of t. To preserve the functions $\sqrt{v_1^2 + k^2}$ and $\sqrt{v_2^2 + k^2}$ single-valued with positive real parts throughout the k-plane, the imaginary axis is cut beyond $\pm iv_1$ for the first integral and $\pm iv_2$ for the second one in each equation of (22), the point $\pm iv_1$ being the lowest one since $v_1 < v_2$. The denominator $\Delta(k)$ in (22) has also a singular point at $\pm iv_r$ on the imaginary axis. Indeed the substitution $k = \pm iv_r$ or $k = \pm i/C$ into expression for $\Delta(k)$ leads to the equation

$$(2 - \alpha C^2/C_T^2)(2 - C^2/C_T^2) = 4\sqrt{(1 - C^2/C_L^2)(1 - C^2/C_T^2)} \qquad (25)$$

which has two real roots $C = \pm C_r$ where $C_r < C_T < C_L$ is a velocity of the surface wave and an expression (25) corresponds to the Rayleigh function for a half-plane. The point $\pm iv_r$ is the highest on the imaginary k-axis. The integrals in (22) have no other singularities. An expression for vertical displacement w will be considered in details below.

The firs integral in the expression for $\bar{w}$ is

$$I_1 = \int_\Gamma \frac{(2k^2 + v_2^2)\sqrt{k^2 + v_1^2}}{\Delta(k)}\, e^{-s(\sqrt{k^2 + v_1^2} \cdot z - ikx)}\, dk \qquad (26).$$

Solving for k the equation (23) gives the following:

$$k = \pm\sqrt{\frac{t^2}{r^2} - v_1^2} \cdot \sin\theta + \frac{it}{r}\cos\theta \tag{27}$$

with $r^2 = x^2 + z^2$ and $\sin\theta = z/r$; $\cos\theta = x/r$; $0 < \theta < \pi$.

Being real and positive the variable t varies from $v_1 r$ to ∞. The variable k traces on the k-plane a hyperbola Γ_1 which cuts the imaginary axis in the point $iv_1 \cos\theta$ (see Fig. 1). Between two curves Γ and Γ_1 there are no singularities and the integrand vanishes at infinity. Both integration paths are equivalent for $0 < \theta < \pi$.

$$I_1 = \int_{v_1 r}^{\infty} \frac{(2k^2 + v_2^2)\sqrt{k^2 + v_1^2}}{\Delta(k)} e^{-st} \frac{\partial k}{\partial t}\, dt \tag{28}$$

and the original function can be written as follows:

$$I(x,z,t) = N_1(k_+)\frac{\partial k_+}{\partial t} - N_1(k_-)\frac{\partial k_-}{\partial t} \tag{29}$$

where $k_\pm$ is defined in (27) and $N_1(k) = \dfrac{(2k^2 + v_2^2)}{\Delta(k)}\sqrt{k^2 + v_1^2}$

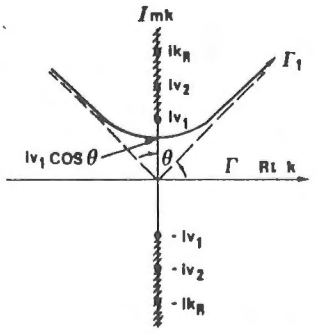

Fig. 1. Path of integration and location of cuts.

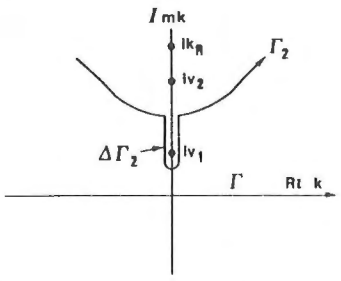

Fig. 2. Path of integration with additional loop.

The second integral is

$$I_2 = \int_{\Gamma} \frac{2k^2 \sqrt{v_1^2 + k^2}}{(k)} e^{-s(\sqrt{v_2^2 + k^2} \cdot z - ikx)} \, dk \qquad (30)$$

Proceeding as previously

$$t = \sqrt{v_2^2 + k^2} \cdot z - ikx \qquad (31)$$

the integration path Γ transforms into Γ_2 along the hyperbola

$$k = \pm \sqrt{\frac{t^2}{r^2} - v_2^2} \cdot \sin\theta + \frac{it}{r} \cos\theta \qquad (32)$$

where t varies from rv_2 to ∞. This time the hyperbola (32) intercepts the imaginary axis at the point $v_2 \cos\theta$. Depending on θ it may happen below iv_1 or between iv_1 and iv_2. In the first case for θ in the range below

$$\arccos \frac{v_1}{v_2} < \theta < \pi - \arccos \frac{v_1}{v_2}$$

the integration paths Γ and Γ_2 are identical as previously and the original function is

$$I_2(x,z,t) = N_2(k_+) \frac{\partial k_+}{\partial t} - N_2(k_-) \frac{\partial k_-}{\partial t} \qquad (33)$$

with $k_\pm$ defined according to (32) and $N_2(k) = \dfrac{2k^2 \sqrt{k^2 + v_1^2}}{\Delta(k)}$ (34)

The second case occurs when θ is in the range

$$0 < \theta < \arccos \frac{v_1}{v_2} \tag{35}$$

Two integration paths Γ and Γ_2 can be made equivalent by adding a loop $\Delta\Gamma_2$ along the imaginary axis and around the point iv_1 (see Fig. 2). This loop consists of a circle of δ radius ($\delta \to 0$) with a centre in iv_1 and two segments of the imaginary axis

$$k = i\left(-\sqrt{v_2^2 - \frac{t^2}{r^2}} \cdot \sin\theta + \frac{t}{r}\cos\theta\right) \pm\delta \tag{36}$$

between the point $iv_2 \cos\theta$ and iv_1. The range of t for this loop is

$$v_2 r < t < v_1 r \cos\theta + r\sqrt{v_2^2 - v_1^2} \cdot \sin\theta \tag{37}$$

$$\text{Then} \quad I_2(x,z,t) = \left[N_2(k_+'') \frac{\partial k_+''}{\partial t} - N_2(k_-'') \frac{\partial k_-''}{\partial t}\right] + f_\theta f_t \left[N_2(k_+''') - N_2(k_-''')\right] \frac{\partial k'''}{\partial t} \tag{38}$$

where k_+'' is defined by (32) and k_+''' by (36).

The factors f_θ and f_t are as follows:

$$f_\theta = \begin{cases} 1 & \text{for } \arccos \frac{v_1}{v_2} < \theta < \pi - \arccos \frac{v_1}{v_2} \\ 0 & \text{otherwise} \end{cases}$$

$$f_t = \begin{cases} 1 & \text{for t in the interval (37)} \\ 0 & \text{otherwise} \end{cases}$$

For θ in the range $\pi - \arccos \frac{v_1}{v_2} < \theta < \pi$ (39)

the hyperbola crosses a negative branch of the imaginary axis and the loop $\Delta\Gamma_2$ will be as below

$$k = \pm\delta + i\left(\sqrt{v_2^2 - \frac{t^2}{r^2}} \cdot \sin\theta + \frac{t}{r}\cos\theta\right) \tag{40}$$

The following expressions define the f-factors

$$f_\theta = \begin{cases} 1 & \text{for } \theta \text{ in the interval (39)} \\ 0 & \text{otherwise} \end{cases}$$

$$f_t = \begin{cases} 1 & \text{for } v_2 r > t > v_2 r\,|\cos\theta| + r\sqrt{v_2^2 - v_1^2}\cdot\sin\theta \\ 0 & \text{otherwise} \end{cases}$$

Finally the vertical displacement due to Dirac impulse applied to the boundary edge is

$$\begin{aligned} w(x,z,t) = {} & \frac{1}{2\pi G}\, U(t - v_1 r)\left[N_1(k_+')\frac{\partial k_+'}{\partial t} - N_1(k_-')\frac{\partial k_-'}{\partial t}\right] \\ & - \frac{1}{2\pi G}\, U(t - v_2 r)\left[N_2(k_+'')\frac{\partial k_+''}{\partial t} - N_2(k_-'')\frac{\partial k_-''}{\partial t}\right] \\ & - \frac{1}{2\pi G}\, f_\theta' f_t' \left[N_2(k_+''') - N_2(k_-''')\right]\frac{\partial k'''}{\partial t} \\ & - \frac{1}{2\pi G}\, f_\theta'' f_t''\left[N_2(k_+'''') - N_2(k_-'''')\right]\frac{\partial k''''}{\partial t} \end{aligned} \tag{41}$$

$$\text{where } N_1(k) = \frac{(2k^2 + v_2^2)\sqrt{k^2 + v_1^2}}{\Delta(k)}$$

$$N_2(k) = \frac{2k^2\sqrt{k^2 + v_1^2}}{\Delta(k)} \tag{42}$$

$$k_{\pm}^{I} = \pm\sqrt{\frac{t^2}{r^2} - v_1^2} \cdot \sin\theta + \frac{it}{r}\cos\theta \quad \text{for } v_1 r < t < \infty$$

and $0 < \theta < \pi$

$$k_{\pm}^{II} = \pm\sqrt{\frac{t^2}{r^2} - v_2^2} \cdot \sin\theta + \frac{it}{r}\cos\theta \quad \text{for } v_2 r < t < \infty$$

and $\arccos\frac{v_1}{v_2} < \theta < \pi - \arccos\frac{v_1}{v_2}$

$$k_{\pm}^{II\,I} = i\left(-\sqrt{v_2^2 - \frac{t^2}{r^2}} \cdot \sin\theta + \frac{t}{r}\cos\theta\right) \pm\delta \quad \text{for } v_2 r < t < v_1 r\cos\theta \tag{43}$$

$$+ \sqrt{v_2^2 - v_1^2} \cdot \sin\theta \quad \text{and} \quad 0 < \theta < \arccos\frac{v_1}{v_2}$$

$$k_{\pm}^{II\,II} = \pm\delta + 1\left(\sqrt{v_2^2 - \frac{t^2}{r^2}} \cdot \sin\theta + \frac{t}{r}\cos\theta\right) \quad \text{for } v_2 r < t < v_2 r\cos\theta$$

$$+ \sqrt{v_2^2 - v_1^2} \cdot \sin\theta \quad \text{and} \quad \pi - \cos\frac{v_1}{v_2} < \theta < \pi$$

Similarly horizontal displacement u(x,z,t) can be found. In this case only the function $N_1(k)$ and $N_2(k)$ will be different.

$$N_1(k) = \frac{ik\,(2k^2 + v_2^2)}{\Delta(k)}$$

$$N_2(k) = -\frac{i2k\sqrt{k^2 + v_1^2}\sqrt{k^2 + v_2^2}}{\Delta(k)} \tag{44}$$

Fig. 3 shows the vertical movement of the surface point close to the applied force. At the time movements rv_1, rv_2 and rv_r the dilatational, distortional and surface wave fronts arrive at this point. A dilatational wave arrives first causing little disturbance. Next comes a slower shear wave which is also very weak and finally the surface wave produces a splash which vanishes almost immediately after the wave has passed by. In other words the splash spreads along the surface from the impact point to infinity preserving its shape and losing its strength.

Fig. 4 shows the surface splash at the distance of 1 m from impact point, and its more detailed configuration can be seen in Fig. 5. The effect of the surface or Rayleigh wave disappears very quickly with growing depth. Under the impact point, no matter how close to the surface, it has no effect at all whereas the most effective is a dilatational wave (see Fig. 6).

The vertical movement of the point (1,1) is shown in Fig. 7 where the shear wave is the strongest.

Although the Navier equation contains no dissipative terms, its solution shows that the impact impulse produces no vibrations. Since there is no reflexion from the nonexisting outer boundaries and therefore no standing waves, the disturbance propagates from the impact point and disappears in infinity leaving almost nothing behind. It means that instead of the internal material friction there exists an energy radiation which can be compared to the damping of the one-degree-of-freedom system.

This form of dynamic response to the impulse excitation can be useful in the flexibility analysis where displacement is sought as a function of the known load time history.

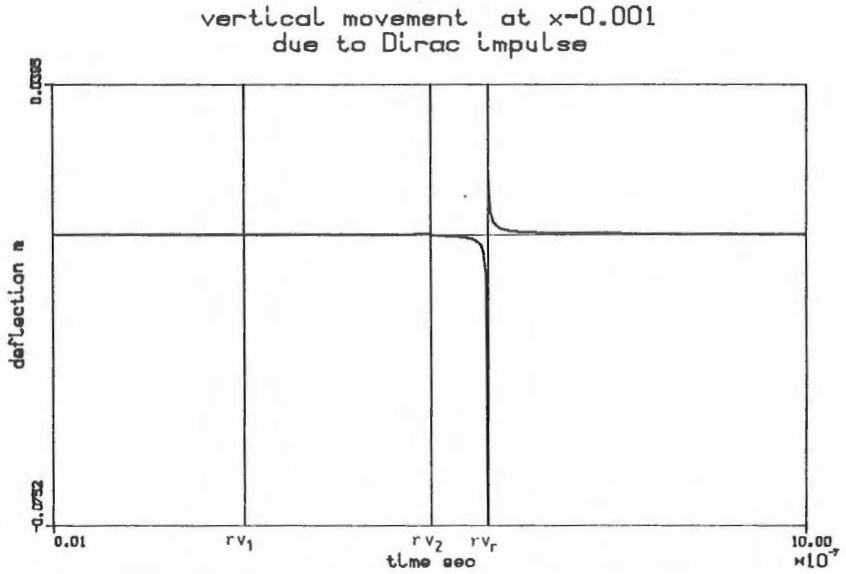

Fig. 3. Vertical movement of the surface point located at the distance of 0.001 m from applied unity impulse. The dilatational, distortional and surface wave fronts pass through this point at the time moments rv_1, rv_2 and rv_r respectively.

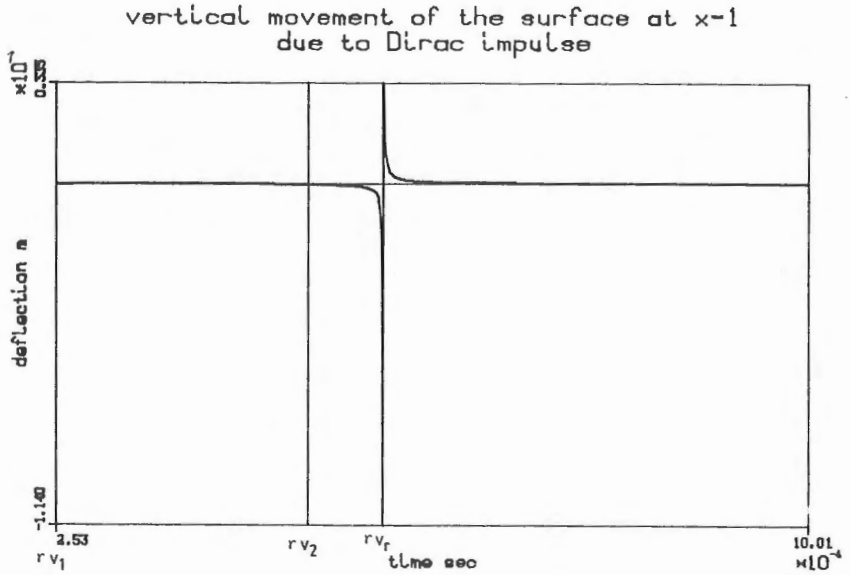

Fig. 4. Vertical movement of the surface point at 1 m from the unity impulse. The amplitude of the splash dropped considerably but its configuration remains unchanged.

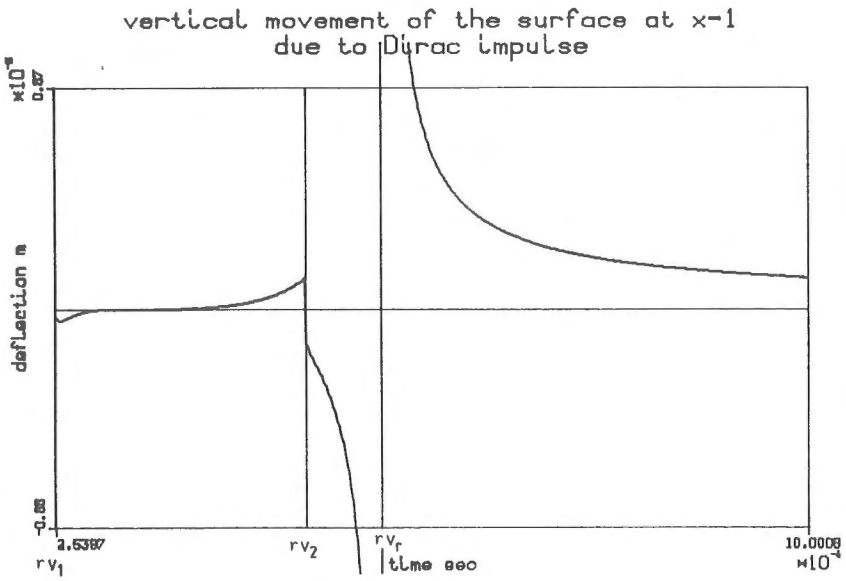

Fig. 5. Detailed configuration of the surface splash cut close to the zero line. The disturbance from the compressive and shear waves after their passage through the point at time moments rv_1, rv_2 is insignificant.

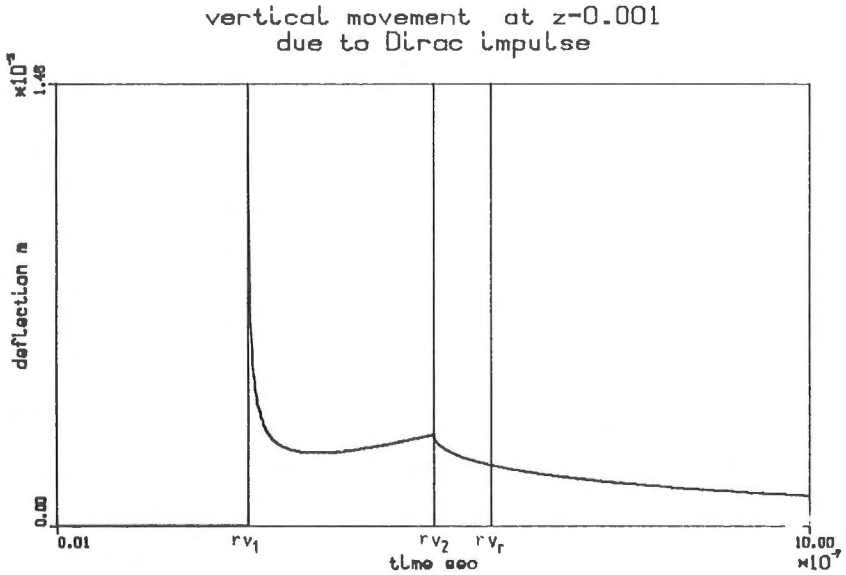

Fig. 6. Vertical movement of the point 0.001 m deep under the impulse. Compressive wave arrives first to this point at time moment rv_1 and causes a splash. Arrival of the Rayleigh wave has no effect at all.

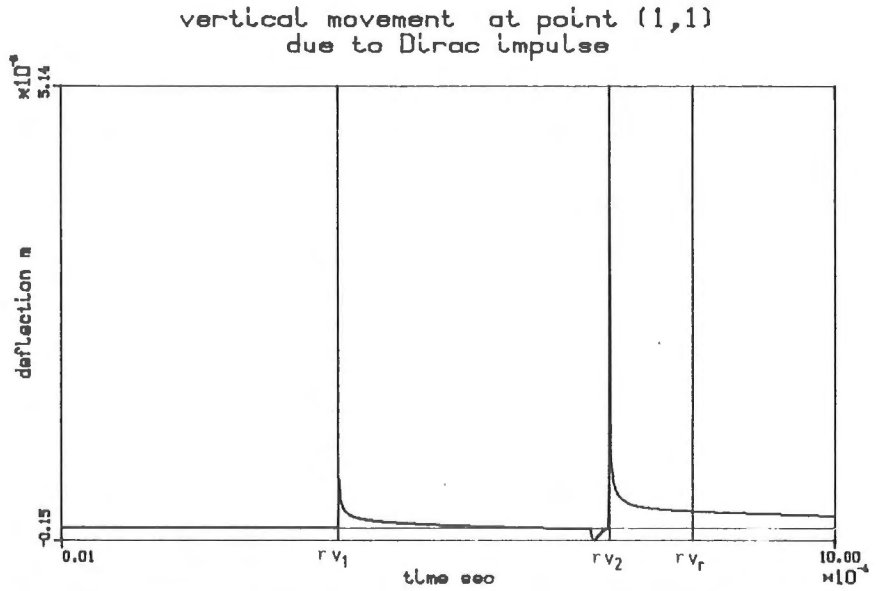

Fig. 7. Vertical movement of the point (1,1). The most significant is a shear wave passage through this point at time moment rv_2. Rayleigh wave leaves no trace passing through the point.

4 Duhamel integral

If there is a solution for an impulse excitation, the dynamic response to the arbitrary force action can be found by using the Duhamel integral

$$w(x,z,t) = \int_0^t P(\tau)\, h(t-\tau)\, d\tau \quad ; \quad h(t) = h(x,z,t) \tag{45}$$

where P(t) is a time history of the concentrated force and h(t) is an impulse response.

It should be noted that although the integration variable is real, it belongs to both real and imaginary parts of a complex variable k in (41) and h(t) defined by (41) is a complex function with a singularity. The real and imaginary parts of h(t) must be integrated

separately. The evaluation of the integral (45) was performed numerically. To distinguish the sharp peaks inside the interval $(v_r - v_1)r$, the time step of 10^{-6} sec was taken within it.

Fig. 8 to 10 present the dynamic response to the unity force applied instantly at t = 0 and remaining for t > 0 on the surface. After a short transient period, the response tends to the static deflection,

$$w_{st} = \lim_{t\to\infty} \int_0^t h(t - \tau)\, d\tau \qquad (46)$$

The figures also reveal the numerical nature of integration: instead of jumping to the static deflection at $t = v_r r$ the curve needs time to reach that level as it does in the analytical solution.

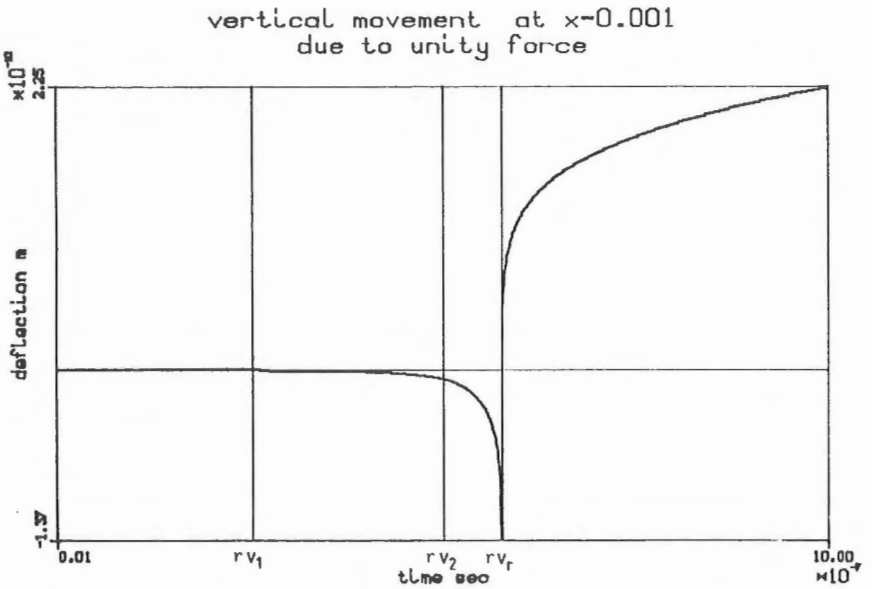

Fig. 8. Vertical movement of the point at 0.001 m from the unity force applied to the boundary edge. rv_1, rv_2 and rv_r are the time moments of the compression, shear and Rayleigh wave passage through the point. Integration step within an interval $r(v_1 - v_r)$ and slightly beyond is 10^{-9} sec.

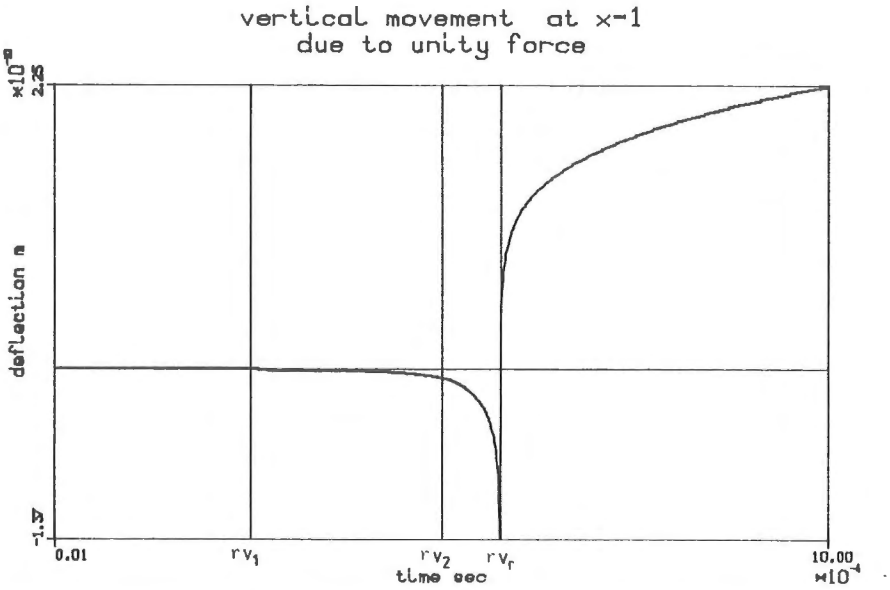

Fig. 9. Vertical movement of the surface point at 1 m from the point of application. Note the same impulse amplitude as in Fig. 8 though the time history considered is 10^3 times longer. Integration step within the same interval is 10^{-6} sec.

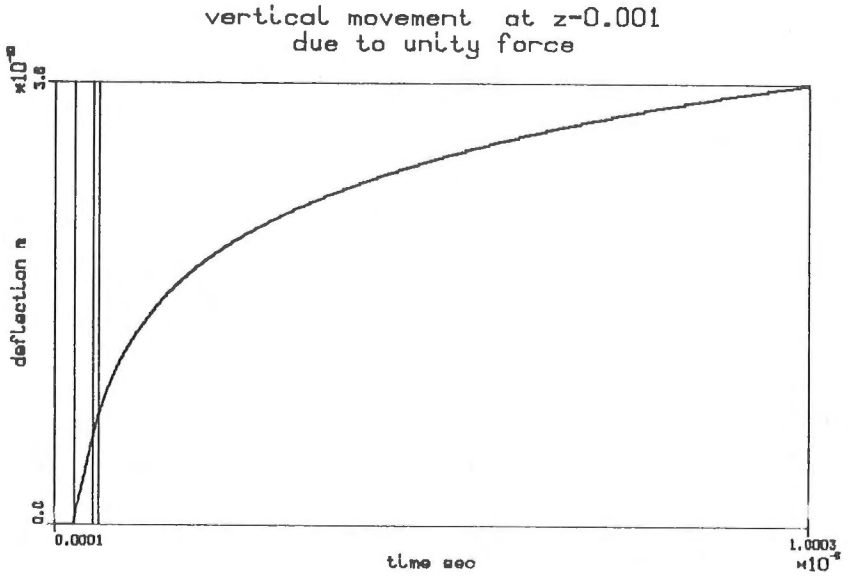

Fig. 10. Vertical movement of the point 0.001 m deep under the unity force. Integration step is 10^{-9} sec throughout the time history.

Observing Fig. 8 and Fig. 9 one may conclude that to follow the sharp and narrow peaks of h(t) inside an interval $r(v_1 - v_r)$, the integration step must be much finer than that of Fig. 8.

5 Dynamic response to the harmonic excitation

Assuming in (44) $P(t) = \sin \omega t$ the response to the harmoic excitation can immediately be found. Fig. 11 to 13 show the vertical movement of the boundary edge in various locations. After the initial splash and short transient period a steady state vibration is established. Fig. 14 to 16 display the vertical movement of the point at various depths under the exciting force. To make steady state movement visible as harmonic one in the neighbourhood of the applied force its frequency ω is chosen fairly high from $4000\,\pi$ to $40000\,\pi$. As it is seen from Fig. 14 arrival of the compression wave triggers oscillations. For comparison, the exciting harmonic force is shown in Fig. 15 as it is at the point of application.

A close observation of these figures reveals the following:

1. The response frequency is higher than that of excitation. The third or forth term in (41), depending on the point locations which are active between the compression and shear wave fronts, represent von Schmidt waves and may be regarded as responsible for the frequency change. According to Huygens principle, the point of intersection of the dilatational front with the boundary can be considered itself as a source of both dilatational and distortional waves thus causing a wave interference in every point within an interval of time $(v_1 - v_r)r$ since the exciting force acts continuously, any border point continuously experiences the passage of the dilatational wave front and therefore is continuously a wave source on its own.

   The response frequency is obviously the same for the whole half-plane.

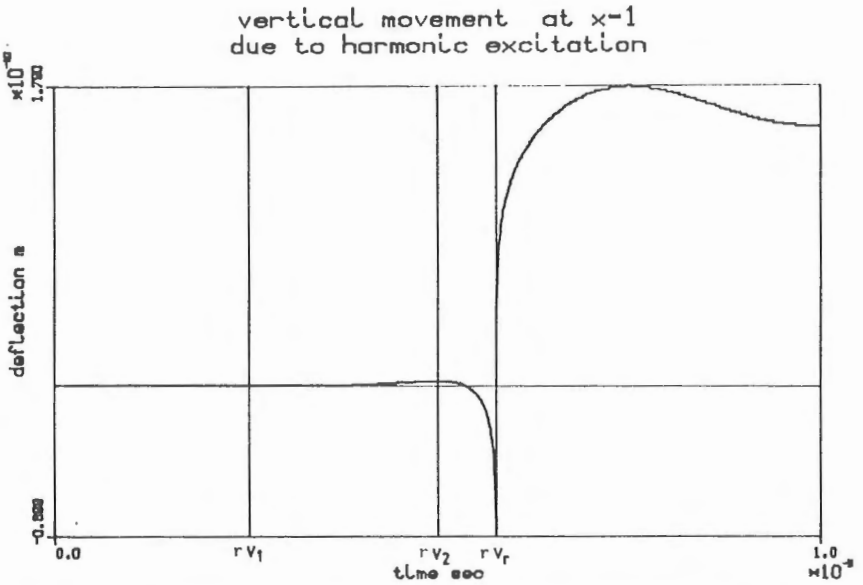

Fig. 11. Vertical movement of the surface point at 1 m from exciting force. Exciting frequency is 4000 π and integration step is 10^{-6} sec. The proper oscillation begins when Rayleigh wave front hits the point and continues afterwards.

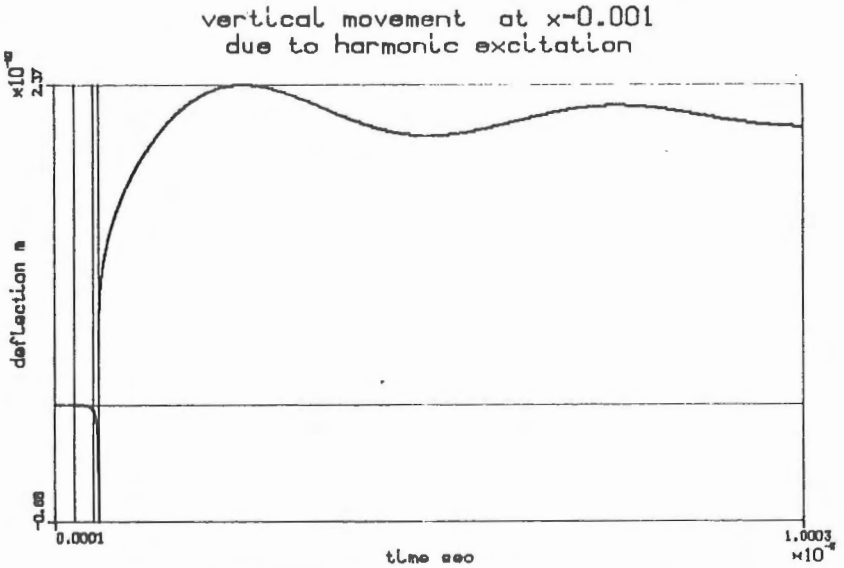

Fig. 12. Vertical movement of the surface point close to the exciting force. Exciting frequency is 400000 π and integration step is 10^{-9} sec.

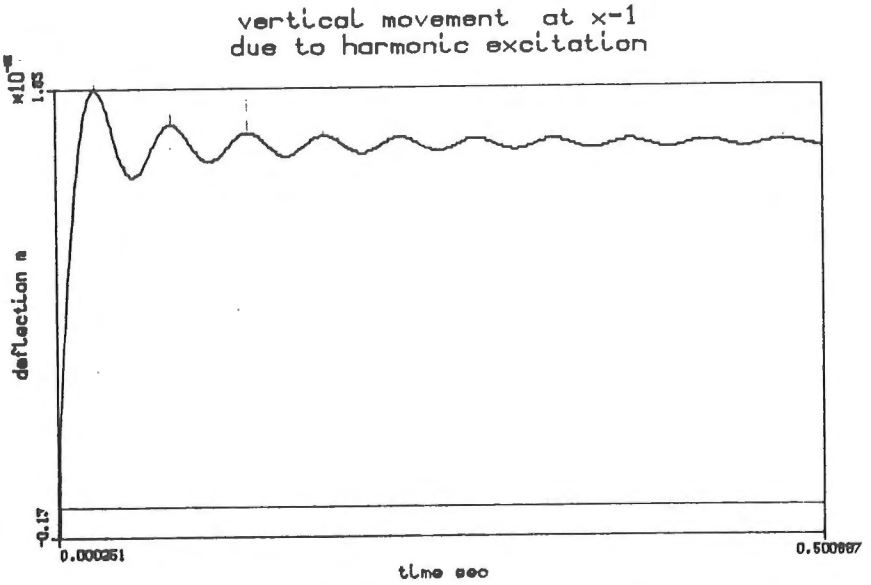

Fig. 13. Vertical movement of the surface point at 1 m from exciting force. Exciting frequency is 40 π and integration step is $(v_i - v_r)/1000$ sec within an interval $(v_i - v_r)r$ and 1/1000 sec beyond it. After a few transient cycles the steady state oscillation is estiablished about a displaces axis.

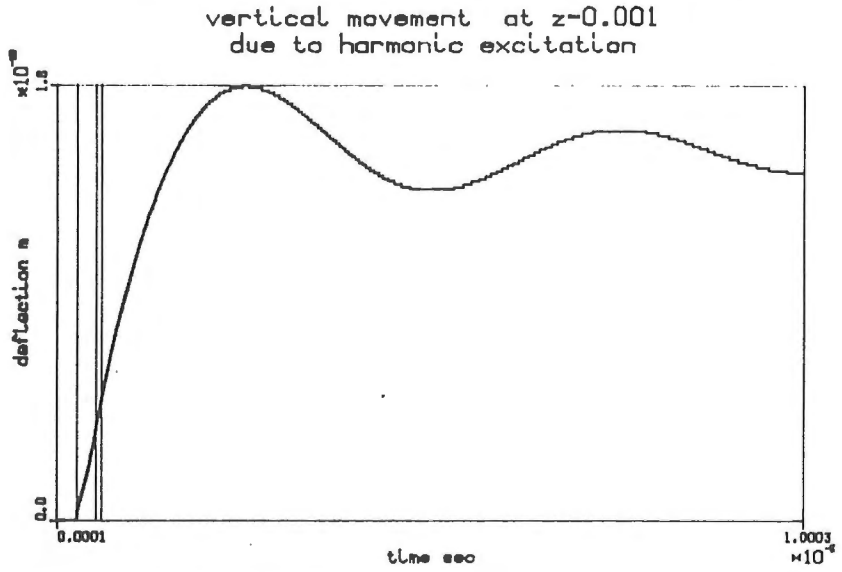

Fig. 14. Vertical movement of the point 0.001 m deep under exciting force. To reveal the oscillating nature of movement during a short time history, the exciting frequency was chosen as 400000 π and the integration step is 10^{-9} sec.

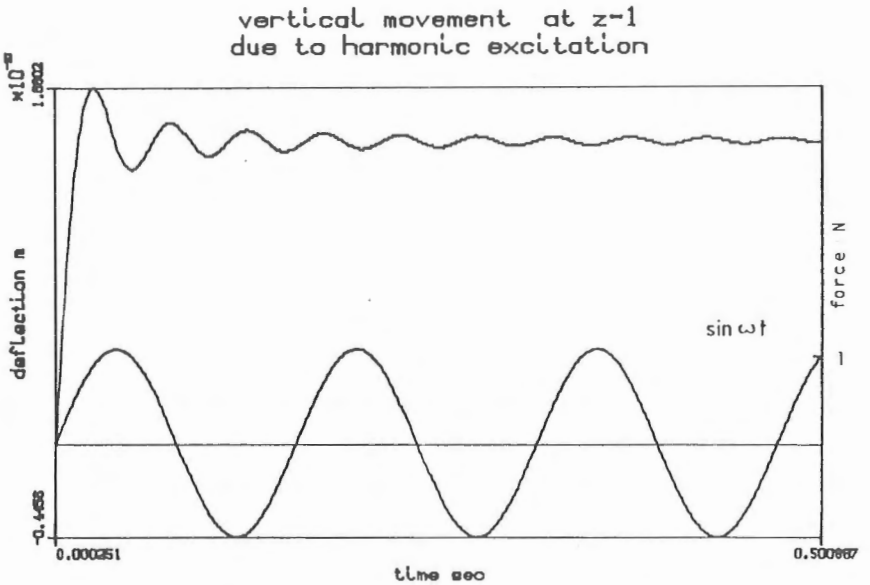

Fig. 15. Vertical movement of the point 1 m deep exciting force. For comparison the excitation is shown beneath the response. Exciting frequency is 40 π and integration step is $(v_1 - v_r)r/1000$ sec within an interval $(v_1 - v_r)r$ and 1/1000 beyond.

2. The amplitude of the response oscillation decreases during a transient period to settle down on a certain level. The impulse function h(t) tends to zero when $t \to \infty$ as fast as 1/t. So for large t the response function will behave as an integral sine Si(t)

$$\lim_{t\to N} \int_0^t \sin \omega t \, h(t - \tau) \, d\tau \Rightarrow \lim_{t\to N} \int_0^t \frac{\sin \omega\tau}{\tau} \, d\tau \Rightarrow Si(t) \qquad (47)$$

where N is a large number.

3. The response displacement function oscillates about a certain constant deflection while the exciting force oscillates about zero. The magnitude and sign of this constant depend on the exciting frequency and location of the vibrating point and may be occasionally zero as well. Indeed the most significant contribution of the impulse function h(t) to Duhamel integral

$$\int_0^t \sin \omega\tau \, h(t - \tau) \, d\tau \tag{48}$$

will be when $v_r + \epsilon < t - \tau < v_1$ (see Fig. 16) for the boundary edge. For other points of the half-plane this interval will be much shorter because of the absence of Rayleigh waves. Corresponding interval for an integration variable τ is

$$t - (rv_r + \epsilon) > \tau > t - v_1 r \tag{49}$$

Changing variables in (48) leads to the following:

$$\begin{aligned} \int_0^t \sin \omega\tau \cdot h(t - \tau) \, d\tau &= -\int_t^0 \sin(\omega t - \omega\xi) \, h(\xi) \, d\xi \\ &= \int_0^t \sin \omega t \cos \omega\xi \, h(\xi) \, d\xi - \int_0^t \cos \omega t \sin \omega\xi \, h(\xi) \, d\xi \end{aligned} \tag{50}$$

First integral in the right hand part of (50) can be presented as follows

$$\int_0^t \sin \omega t \cos \omega\xi \, h(\xi) \, d\xi = \int_0^{rv_1} + \int_{rv_1}^{rv_r+\epsilon} + \int_{rv_r+\epsilon}^t$$

Integral $\int_0^{rv_1}$ = 0 since no wave front arrives to the point of consideration. Integral $\int_{rv_1}^{rv_r+\epsilon}$ gives a constant. The interval $rv_1 + \epsilon)$ depends on the location of the vibrating point. In the neighbourhood of the exciting force this interval is very short and the factor sin ωt does not alter the constant much unless the frequency ω is very high. For the points far away from the origin this interval will be larger and the factor sin ωt may change the constant considerably.

$$\sin \omega rv_1 \int_{rv_1}^{rv_r+\epsilon} \cos \omega\xi \, h(\xi) \, d\xi < \int_{rv_1}^{rv_r+\epsilon} \sin \omega t \cos \omega t \, h(\xi) \, d\xi$$

$$< \sin \omega (rv_r + \epsilon) \underbrace{\int_{rv_1}^{rv_r+\epsilon} \cos \omega\xi \, h(\xi) \, d\xi}_{C_1}$$

Integral $\int_{rv_r+\epsilon}^{t}$ is a time function of the Si(t) type. Together with sin ωt it produces a low amplitude oscillation about the constant C_1 with the response frequency different from ω. The second integral in the right hand part of (50) can be treated similarly. Finally for $t > rv_r + \epsilon$ the upper boundary of the expression (50) can be rewritten as follows:

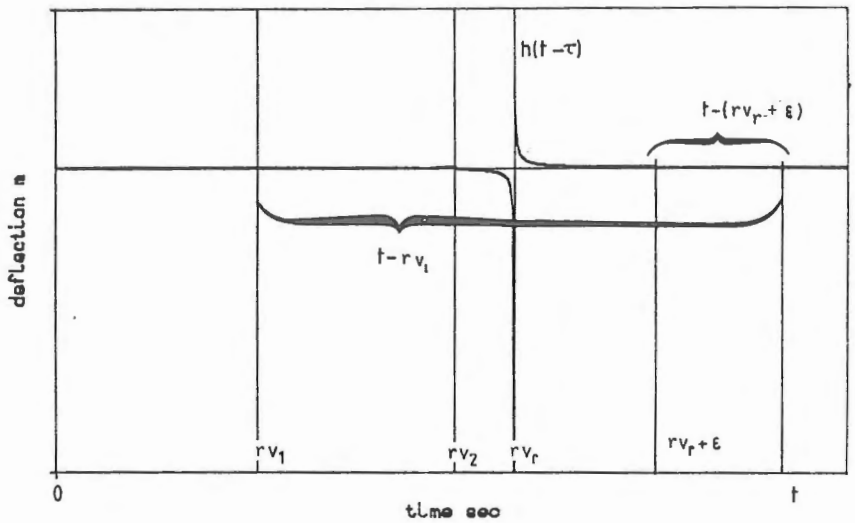

Fig. 16. Interval for the argument $(t - \tau)$ where $h(t)$ contributes the most to the Duhamel integral. Beyond $rv_r + \epsilon$ the impulse function $h(t)$ decreases smoothly no faster than $1/t$. Parameter ϵ can be about 0.1 rv_r or less.

$$\int_0^t \sin \omega\tau \, h(t - \tau)d\tau = \sin (rv_r + \epsilon)C_1 + \int_{rv_r+\epsilon}^t \sin \omega t \cos \omega\xi \, h(\xi)d\xi$$

$$- \cos (rv_r + \epsilon)C_2 - \int_{rv_r+\epsilon}^t \cos \omega t \sin \omega\xi \, h(\xi)d\xi \qquad (51)$$

$$= C + \int_{rv_r+\epsilon}^t \sin \omega t \cos \omega\xi \, h(\xi)d\xi - \int_{rv_r+\epsilon}^t \cos \omega t \sin \omega\xi \, h(\xi)d\xi$$

where $C = \sin \omega (rv_r + \epsilon)C_1 - \cos \omega (rv_r + \epsilon)C_2$.

Fig. 17 shows a case when the constant C is negative. It should be noted however that C is constant for a particular point only and changes with the coordinates. Indeed putting a value for rv_r as the time needed for a surface wave to reach this point one will have

$$C = \sin \omega \left(\frac{r}{C_r} + \epsilon\right) \int_{r/C_L}^{r/C_r+\epsilon} \cos \omega\xi \; h(\xi)d\xi - \cos \omega \left(\frac{r}{C_r} + \epsilon\right) \int_{r/C_L}^{r/C_r+\epsilon} \sin \omega\xi \; h(\xi)d\xi \tag{52}$$

where r is radius-vector of the point of consideration, $r^2 = x^2 + z^2$. For z = 0 the expression (52) defines the shape of the boundary edge about which the small oscillations occur. It has the same structure as (51) and forms a kind of a standing sine wave. For points under the exciting force (x = 0) the wave velocity C_r could be replaced by C_T in (51) and (52).

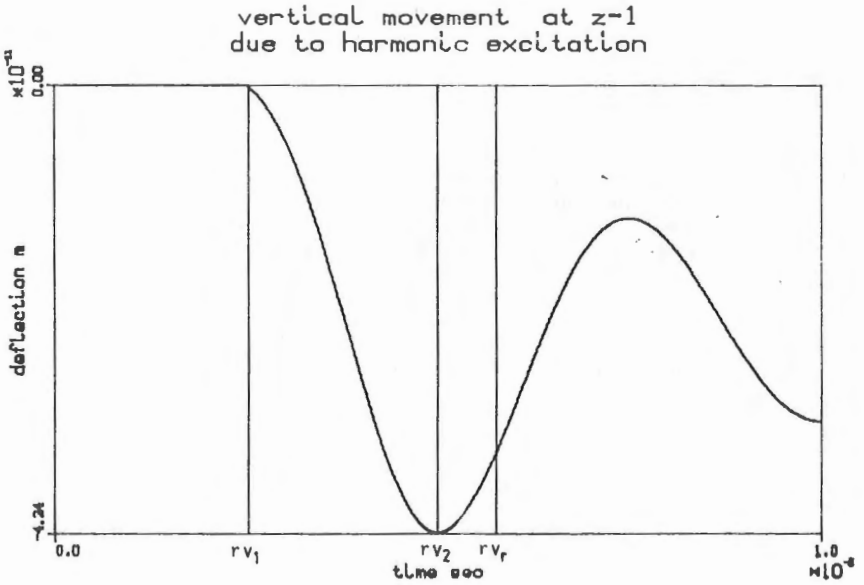

Fig. 17. Vertical movement of the point 1 m deep under exciting force. Exciting frequency is 4000 π and integration step is 10^{-6} sec. The arrival of a compression wave front triggers oscillations at the time moment rv_1 and after few cycles the process goes on about the certain negative depression. In an actual coordinate system, negative direction means an outward one reltive to the half-plane.

6 Geometrical damping

The energy dissipated in the process by outgoing waves can be estimated by

the work done by the exciting force on harmonic motion over a whole cycle.

$$A = \int_0^{2\pi/\omega} \sin \omega t \, \frac{\partial}{\partial t} \int_0^t \sin \omega\tau \, h(t - \tau) \, d\tau dt \tag{53}$$

Integration by parts of (53) yields

$$A = -\omega \int_0^{2\pi/\omega} \cos \omega t \int_0^t \sin \omega\tau \, h(t - \tau) \, d\tau dt \tag{54}$$

As seen from the oscillation figures, the response frequency differs from tht of excitation and judging by (51) there is a phase shift β between excitation and response. So for steady state vibrations the relation (54) will be as follows

$$\begin{aligned} A &= -a\omega \int_0^{2\pi/\omega} \cos \omega t \sin (\omega_1 t + \beta) \, dt \\ &= a \frac{1}{1 - \alpha^2} \cos \beta \, (\cos 2\pi\alpha - 1) + \frac{\alpha a}{1 - \alpha^2} \sin \beta \sin 2\pi\alpha \end{aligned} \tag{55}$$

where $\alpha = \frac{\omega_1}{\omega}$ and a is a response amplitude. If α is not equl to an integer, the work done over the whole cycle, and therefore the energy loss, will depend on this ratio α and phase shift β. The amount of dissipated energy estimated in (55) reflects the dynamic damping properties of the half-plane.

7 Dynamic response to the deflection impulse

Consider now the situation when a unit vertical deflection w = 1 is applied instantly to the point of origin at the time moment t = 0 and then for t > 0 the point of origin is kept at zero. In other words instead of the impulse force an impulse deflection is applied to the origin point which afterwards retains a zero position.

The boundary condition (10) in this case take the following form:

$$\sigma_{zx}\Big|_{z=0} = 0 \; ; \; \sigma_{zz}\Big|_{z=0} = \delta(x)\, F(t) \; ; \; w\Big|_{\substack{x=0\\z=0}} = \delta(t) \tag{56}$$

where F(t) is an unknown force at the origin needed to maintain its position at zero for t > 0. The delta-function $\delta(x)$ keeps the boundary edge free. Applying Laplace transformation to (56) and introducing two potential functions as befor yields the following

$$\begin{aligned}
&2\frac{\partial^2}{\partial x \partial z}\bar{\Phi} + \frac{\partial^2}{\partial x^2}\bar{\psi} - \frac{\partial^2}{\partial z^2}\bar{\psi} = 0 \quad ; \quad z = 0 \\
&\lambda\frac{(1-2\mu)}{1-\mu}\Delta\bar{\Phi} + 2G\left(\frac{\partial^2}{\partial z^2}\bar{\Phi} + \frac{\partial^2}{\partial x \partial z}\bar{\psi}\right) = \delta(x)\,\bar{F}(s) \quad ; \; z = 0 \\
&\frac{\partial}{\partial z}\bar{\Phi} + \frac{\partial}{\partial x}\bar{\psi} = 1 \quad ; \; z = 0 \quad ; \quad x = 0
\end{aligned} \tag{57}$$

where $\bar{\Phi}$ and $\bar{\psi}$ are defined by the expressions (15).

As previously the first condition of (64) gives

$$P_1(k) = (2k^2 + v_2^2)\, R(k) \quad ; \quad P_2(k) = -2ik\sqrt{v_1^2 + k^2}\, R(k) \tag{58}$$

The unknown function R(k) is sought from the third condition of (57)

$$-\int_{\Gamma} v_2^2 \sqrt{v_1^2 + k^2}\, R(k)\, s\,dk = 1 \tag{59}$$

Recalling that the path of integration Γ goes along the real k-axis, the unity in the right hand part of (59) can be presented as follows

$$1 = \int_{\Gamma} f(k)\, dk = \int_{-\infty}^{\infty} f(k)\, dk = \frac{1}{\sigma\sqrt{\pi}} \int_{-\infty}^{\infty} e^{-\frac{k^2}{\sigma^2}}\, dk \tag{60}$$

and equation (60) transforms into the following:

$$-\int_{\Gamma} v_2^2 \sqrt{v_1^2 + k^2}\, sR(k)\, dk = \int_{\Gamma} f(k)\, dk \tag{61}$$

where $f(k) = \dfrac{e^{-k^2/\sigma^2}}{\sigma\sqrt{\pi}}$.

Parameter $\sigma = 1$ s/m ensures the proper dimensions of (60). Solving (68) for R(k) gives

$$R(k) = \frac{-f(k)}{sv_2^2 \sqrt{v_1^2 + k^2}} \tag{62}$$

The potential transforms are now as follows:

$$\bar{\Phi} = \int_{\Gamma} (2k^2 + v_2^2)\, \frac{f(k)}{sv_2^2 \sqrt{v_1^2 + k^2}}\, e^{\zeta}\, dk$$

$$\bar{\psi} = i\int_{\Gamma} \frac{2k}{sv_2^2}\, f(k)\, e^{\eta}\, dk \tag{63}$$

where ζ and η are defined by (22*).

Correspondingly the displacement transforms (22) now like the following:

$$\bar{u} = -i \int_\Gamma \frac{k\,(2k^2 + v_2^2)}{v_2^2\,\sqrt{v_1^2 + k^2}}\, f(k)\, e^{\zeta}\, dk - i \int_\Gamma 2k\,\sqrt{v_2^2 + k^2}\, f(k)\, e^{\eta}\, dk$$

$$\bar{w} = \int_\Gamma \frac{1}{v_2^2}\,(2k^2 + v_2^2)\, f(k)\, e^{\zeta}\, dk - \int_\Gamma \frac{1}{v_2^2}\, k^2\, f(k)\, e^{\eta}\, dk \tag{64}$$

Following the same reasoning as previously the displacements $w(x,z,t)$ and $u(x,z,t)$ will be defined by (41) where the factor $1/2\pi G$ is changed for $2\pi G$ and the function $N_1(k)$ and $N_2(k)$ are as follows:

$$\left.\begin{aligned} N_1(k) &= \frac{1}{v_2^2}\,(2k^2 + v_2^2)\, f(k) \\ N_2(k) &= \frac{1}{v_2^2}\, 2k^2\, f(k) \end{aligned}\right\} \text{for vertical displacement } w$$

$$\left.\begin{aligned} N_1(k) &= -ik\,\frac{(2k^2 + v_2^2)}{v_2^2\,\sqrt{v_1^2 + k^2}}\, f(k) \\ N_2(k) &= 2ik\,\sqrt{v_2^2 + k^2}\, f(k) \end{aligned}\right\} \text{for horizontal displacement } u \tag{65}$$

Using the expression (20) for Dirac delta-function the second condition in (57) can be written as follows:

$$-\lambda\alpha \int_\Gamma \frac{v_1^2}{v_2^2} f(k)\,\frac{2k^2 + v_2^2}{\sqrt{v_1^2 + k^2}} e^{\zeta} dk - 2G \int_\Gamma \frac{1}{v_2^2}\,(2k^2 + v_2^2)\sqrt{v_1^2 + k^2}\, f(k) e^{\zeta} dk$$

$$+ 2G \int_\Gamma \frac{1}{v_2^2}\, 2k^2\,\sqrt{v_2^2 + k^2}\, f(k) e^{\eta} dk = \frac{1}{2\pi s} \int s\bar{F}(s) e^{iksx} dk \text{ on } z = 0 \tag{66}$$

Here as previously $\alpha = \dfrac{1 - 2\mu}{1 - \mu}$.

The inverse transform of the left part of (66) can be found by Cagniard method using expression (41) with

$$N_1(k) = -\lambda\alpha \frac{v_1^2}{v_2^2} f(k) \frac{2k^2 + v_1^2}{\sqrt{v_1^2 + k^2}} - 2G \frac{1}{v_2^2} (2k^2 + v_2^2) \sqrt{v_1^2 + k^2}\, f(k)$$

$$N_2(k) = 2G \frac{2k}{v_2^2} \sqrt{v_2^2 + k^2}\, f(k) \qquad (67)$$

and changing the factor $1/2\pi G$ for 1. Thus for the right hand of (66) $\dfrac{\bar{F}(s)}{s}\,\delta(x)$ the inverse Laplace transform R(x,z,t) was found using expressions (41) and 67).

$$\delta(x) \frac{\bar{F}(s)}{s} \div R(x,z,t)\Big|_{z=0} \qquad (68)$$

The inverse Laplace transform of the left hand part of (68) will be

$$\delta(x)\, F(t) = \int_0^t R(x,z,t)\Big| dt$$

or (69)

$$F(t) = \delta(x) \int_0^t R(x,z,t)\Big| dt_{z=0}$$

The delta-function filters the integral in (69) along the x-axis so that it has a meaning only in x = 0 thus making the reaction force F(t) only a time function. Practically the delta-function is used as a limit (19). Then

$$F(t) = \lim_{\substack{\epsilon\to 0 \\ \beta\to 0}} \frac{1}{\epsilon}\left[U\left(x+\frac{\epsilon}{2}\right) - U\left(x-\frac{\epsilon}{2}\right)\right] \int_0^t R(x,z,t)\,dt\Big|_{z=0} = \lim_{\substack{\epsilon\to 0 \\ \beta\to 0}} \frac{1}{\epsilon}\left[e^{-\beta\left(x+\frac{\epsilon}{2}\right)} - e^{-\beta\left(x-\frac{\epsilon}{2}\right)}\right] \int_0^t R(x,z,t)\,dt\Big|_{z=0} \tag{70}$$

This form of dynamic solution provides an influence or Green function for a Duhamel integral used in stiffness analyses.

Fig. 18 to 20 present the dynamic response to the deflection impulse applied at the origin for different locations within the half-plane.

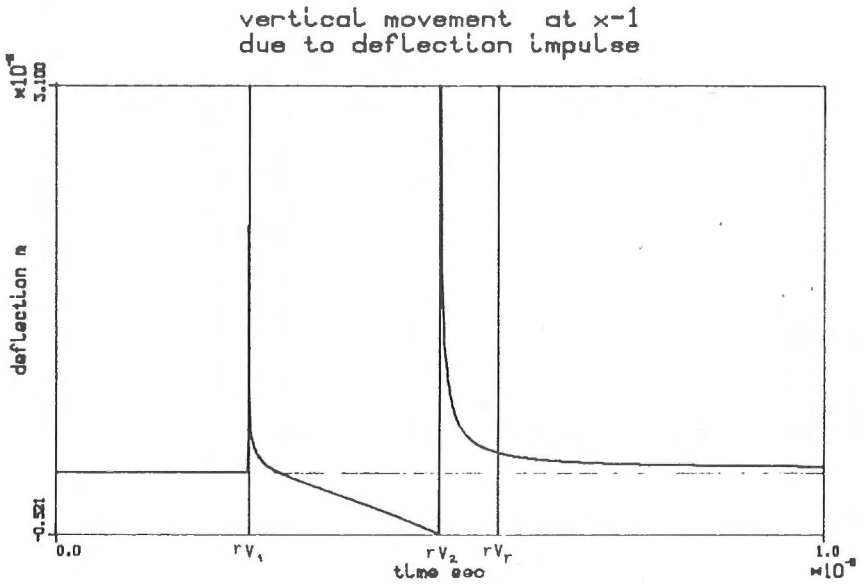

Fig. 18. Dynamic response to the deflection impulse at the boundary edge. There is no Rayleigh wave effect seen at the time moment rV_r.

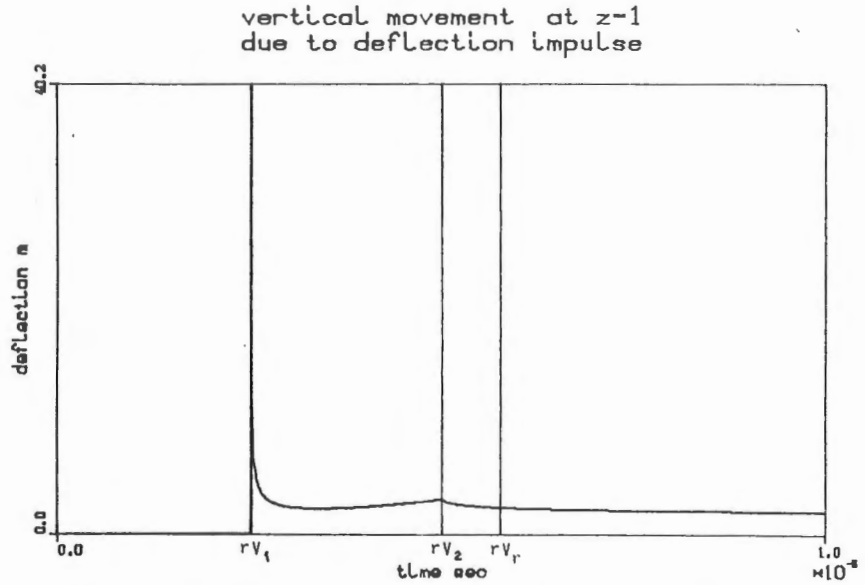

Fig. 19. Dynamic response to the deflection impulse under its point of application. The dilatational wave effect prevails.

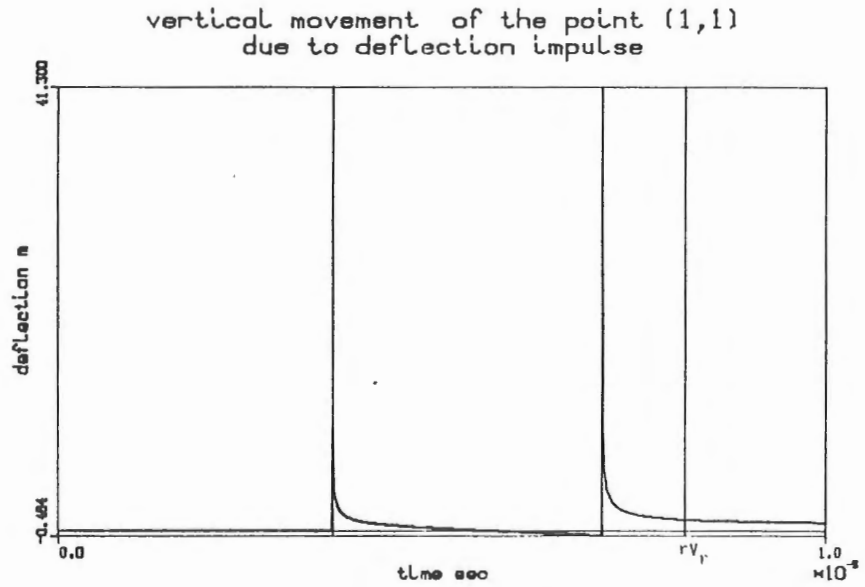

Fig. 20. Dynamic response to the deflection impulse at the point (1,1) of the half-plane.

8 Conclusions

It is necessary, according to many researchers, to include in the ice-structure interaction model the dynamic behaviour of the moving ice sheet. It should also be taken into account when analyzing the field record data. For slender structures the simple mecanical ice sheet model with equivalent dissipating ability may be employed. For larger structures with contact area spread at random along the ice-structure interface, a two-dimensional option should be used in its flexibility of stiffness from depending on the mode of solution of governing interaction equations.

9 References

Kärnä T. and Turunen R., Dynamic response of narrow structures to ice crushing. Cold Regions Science and Technology. 1989. (in press)
Määttänen M., Ice-induced vibrations of structure; self-excitation. IAHR, Sapporo, Japan, 1988.
Sodhi D., Ice-induced vibrations of structures. IAHR, Sapporo, Japan, 1988.
Fung Y.C., Foundation of solid mechanics. Prentice-Hall Int., 1965.
Biggs J. Introduction to structural dynamics. McGroc-Hill Book Co, 1964.

Juri Kajaste-Rudnitski, tutkija, Valtion teknillinen tutkimuskeskus. Rakennetekniikan laboratorio.